Electronic Supplementary Material (ESI) for Physical Chemistry Chemical Physics.

SUPPORTING INFORMATION

Revealing Light-Induced Structural Shifts in G-Quadruplex-Porphyrin Complexes: A Pulsed Dipolar EPR Study

Natalya E. Sannikova,[a,b] Mikhail I. Kolokolov,[a,b] Tamara A. Khlynova,[a,b] Alexey S. Chubarov,[c,b] Yuliya F. Polienko,[d] Matvey V. Fedin,[a,b*] and Olesya A. Krumkacheva[a,b*]

[a] International Tomography Center SB RAS, 630090 Novosibirsk, Russia

[b] Novosibirsk State University, Pirogova Str. 2, Novosibirsk 630090, Russia

[c] Institute of Chemical Biology and Fundamental Medicine SB RAS, Novosibirsk 630090, Russia

[d] N.N. Vorozhtsov Institute of Organic Chemistry SB RAS, 630090 Novosibirsk, Russia

* Email addresses: olesya@tomo.nsc.ru (O.A.K), mfedin@tomo.nsc.ru (M.V.F.)

Table of contents

1. UV-Vis absorption spectra of the HTel-22/TMPyP4 complex and irradiation spectrum of light-emitting diode (LED)

Figure S1 demonstrates absorption spectra of HTel-22/TMPyP4 complex and the irradiation spectra of the diode used in this study in arbitrary units.

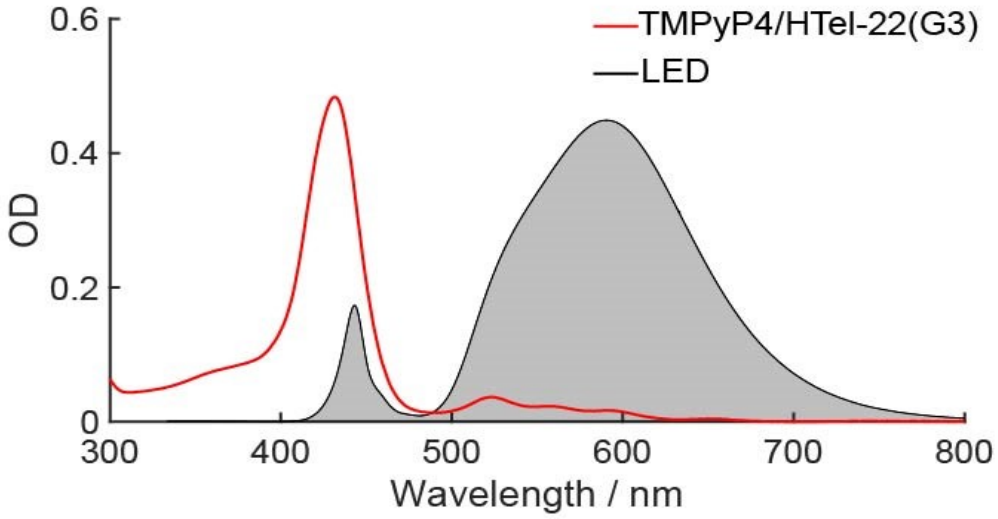

Figure S1. UV-VIS absorption spectra of singly labeled TMPyP4/HTel-22(G3) complex ([HTel-22]=2 μM, [TMPyP4]=4 μM) at concentration ratio 2:1 in 10 mM Tris-HCl buffer with 100 mM KCl (red line). The irradiation spectra of the diode, represented in arbitrary units, are illustrated as a black line with a gray shaded area.

2. Data processing of LaserIMD measurements of TMPyP4/HTel-22(G3).

The choice of baseline function fitting model can significantly impact distance distribution results. Figure S2 illustrates ReLaserIMD data processing, assuming a standard homogeneous three-dimensional exponential background. As can be seen in Fig. 2a, this three-dimensional exponential background does not accurately represent the experimental data. Background-corrected traces display long oscillations that lead to artifact peaks at long distances (~5.3 nm), surpassing the calculated distances for the investigated complex. The non-exponential behavior of the background function is likely attributed to significant influences of excluded volume effects [1]. To avoid these artifact oscillations in data analysis, we employed a 3rd order polynomial background for all dipole experiments, in conjunction with the Tikhonov regularization procedure (Fig. S3, Fig. S4).

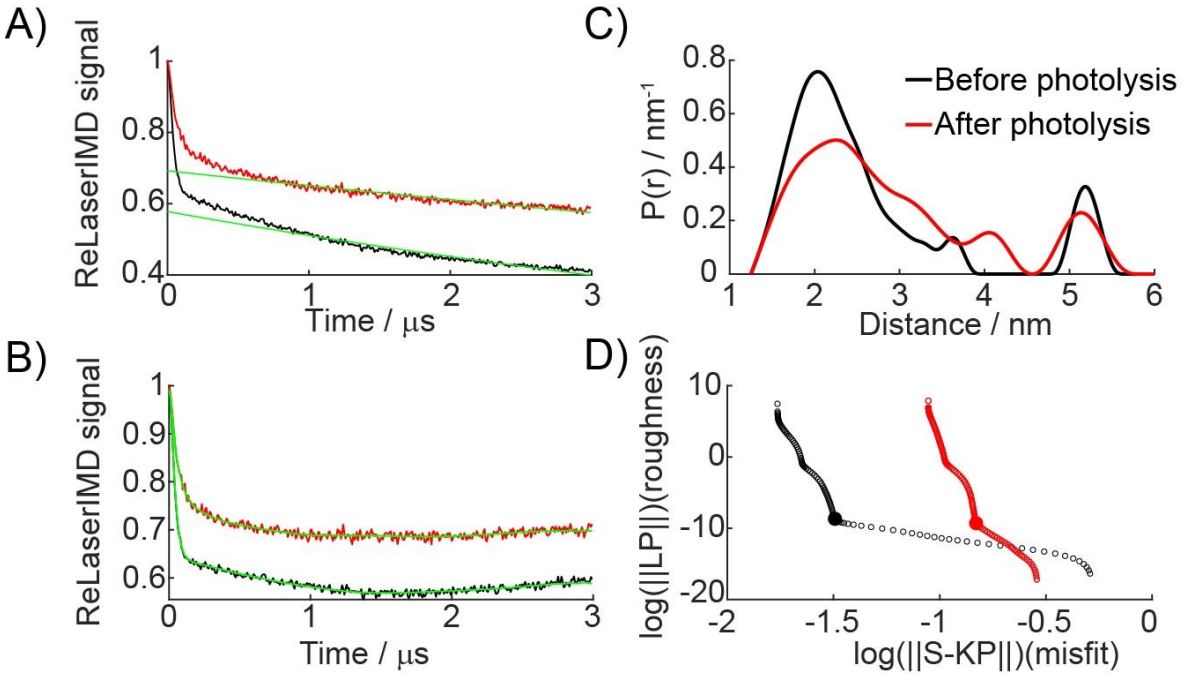

Figure S2. Q-band ReLaserIMD measurements of TMPyP4/ HTel-22 (G3) complex at 30K before (black lines) and after (red lines) photolysis for 60 min with exponential background fits. A) The original time traces and their background fits colored green B) Background corrected dipolar evolution data and their best-fit curves using Tikhonov regularization corresponding to the AIC criteria (green). C) Computed distance distribution profiles normalized on modulation depth. D) The calculated L-curves. The choice of α are also indicated.

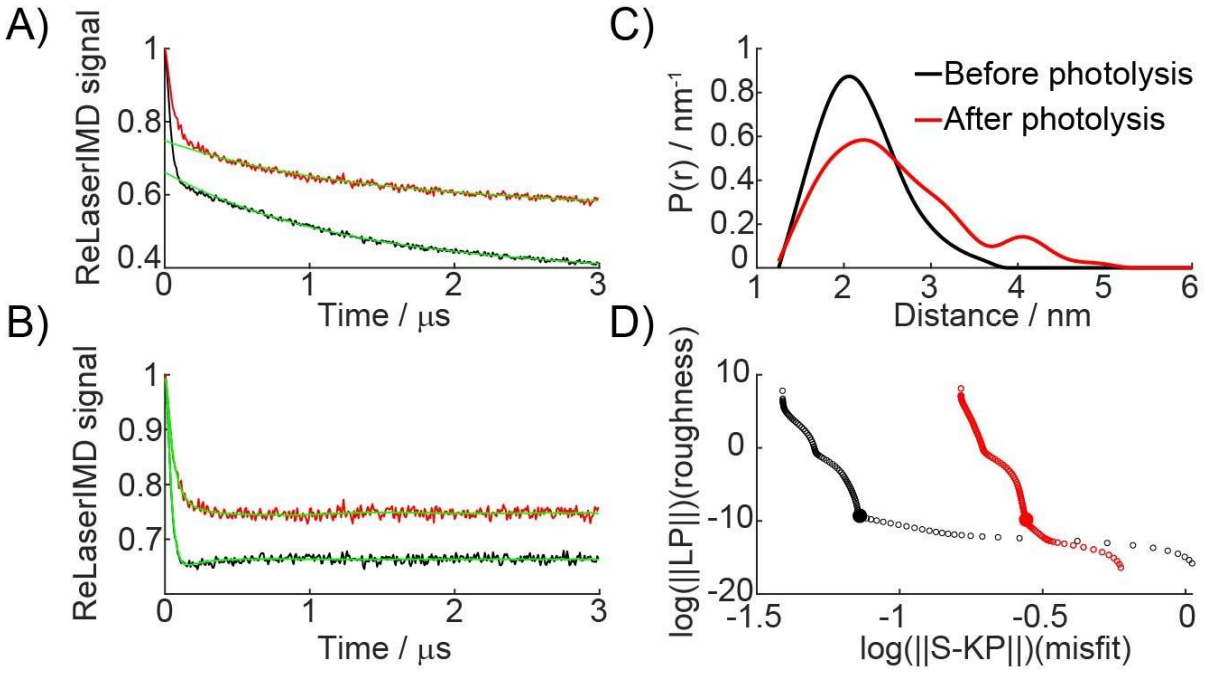

Figure S3. Q-band ReLaserIMD measurements of TMPyP4/ HTel-22 (G3) complex at 30K before (black lines) and after (red lines) photolysis for 60 min with 3th-order polynomial

background fits. A) The original time traces and their background fits colored green B) Background corrected dipolar evolution data and their best-fit curves using Tikhonov regularization corresponding to the AIC criteria (green). C) Computed distance distribution profiles normalized on modulation depth. D) The calculated L-curves. The choice of α are also indicated.

3. Data processing of DEER data

Figure S4 compares DEER measurements between two nitroxide labels of TMPyP4/HTel-22(G3) using Tikhonov regularization.

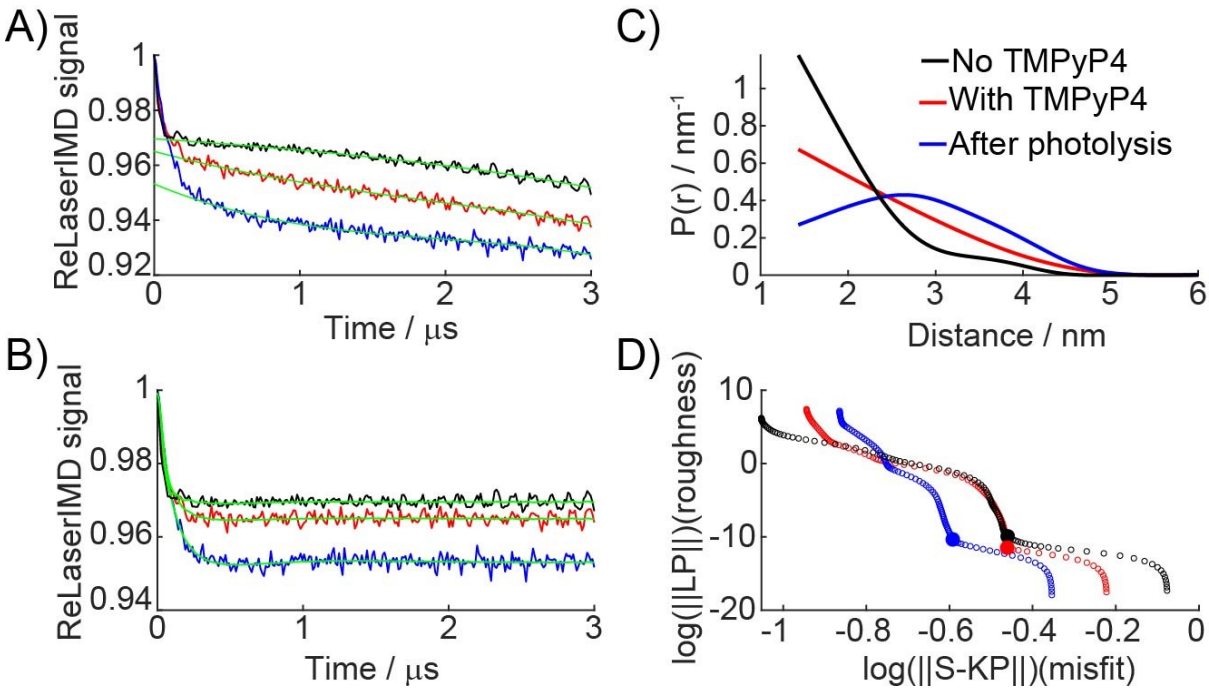

Figure S4. Q-band DEER measurements of HTel-22 (G3) at 50 K in the absence of TMPyP4 (black lines), in complex with TMPyP4 before (red lines) and after (blue lines) photolysis for 60 min with 3th-order polynomial background fits. A) The original time traces and their background fits colored green B) Background corrected dipolar evolution data and their best-fit curves using Tikhonov regularization corresponding to the AIC criteria (green). C) Computed distance distribution profiles normalized on modulation depth. D) The calculated L-curves. The choice of α are also indicated.

Figure S5 compares DEER measurements between two nitroxide labels of TMPyP4/HTel-22(G3; G15) using DEERNet approach.

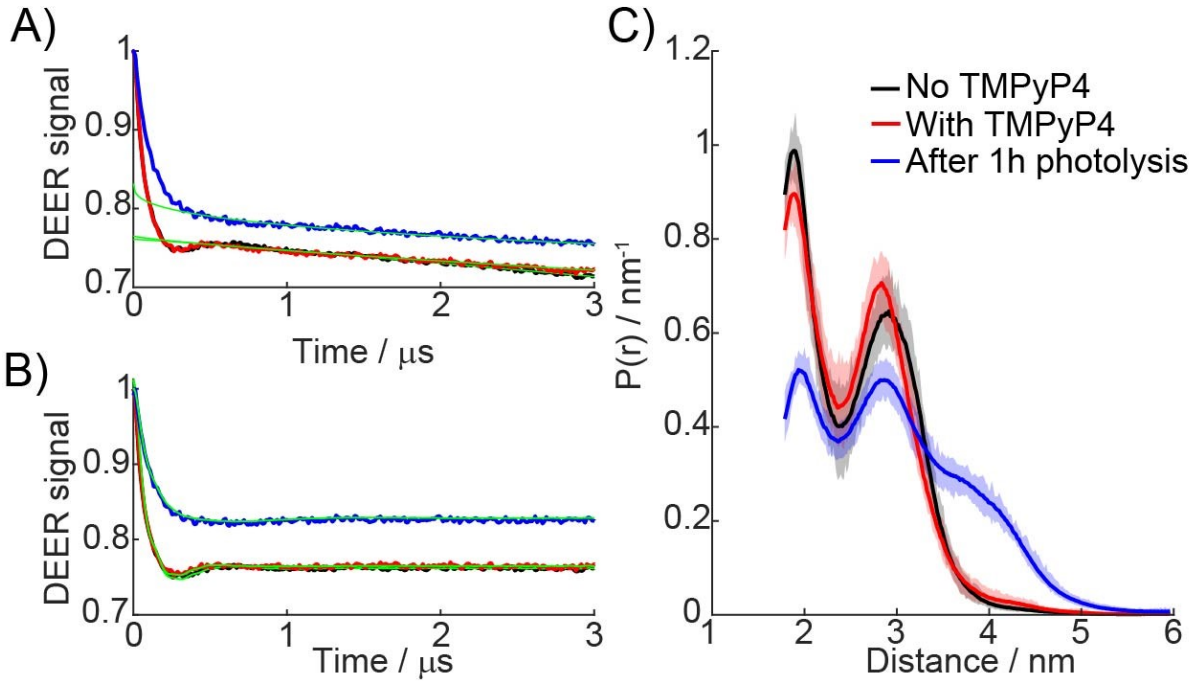

Figure S5. Q-band DEER measurements of HTel-22 (G3; G15) at 50K without TMPyP4 (black lines), in the complex with TMPyP4 before (red lines) and after (blue lines) photolysis for 60 min. A) The original time traces and their background fits colored green B) Background corrected dipolar evolution data and their best-fit curves using DEERNet software C) Computed distance distribution profiles normalized on modulation depth.

4. UV-Vis spectroscopy titration

Figure S6 compares the changes in UV-Vis absorption spectra of wild-type DNA and its spin-labeled derivatives as the concentration of HTel-22 increases.

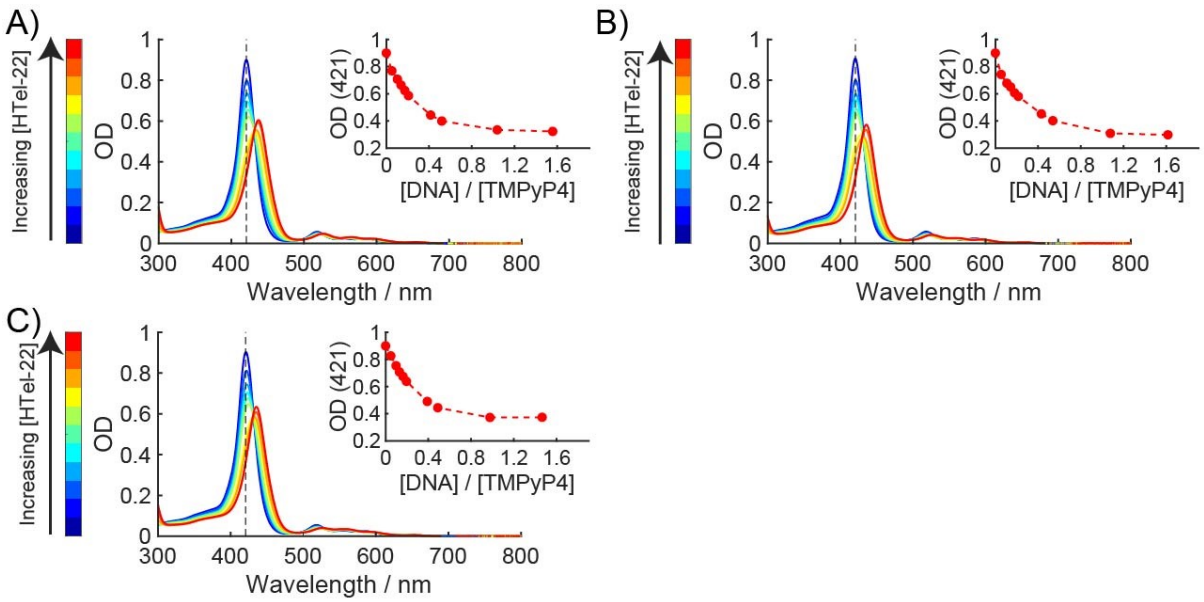

Figure S6. UV− Vis absorption spectra of TMPyP4 as a function of wt HTel-22 (A) and its spin derivatives concentration: HTel-22 (G3) (B) and HTel-22 (G3; G15) (C) concentration. The TMPyP4 concentration was 4 μM, while DNA concentrations range from 0 to 6 μM. Inserted figures indicate the decreasing optical density at 421 nm.

5. ED spectra before and after irradiation

Figure S7 demonstrates the echo-detected (ED) spectra of the studied samples before and after 1h photolysis which indicate the ~30% reduction in the overall photoexcited triplet state concentration after 60 min continuously photolysis.

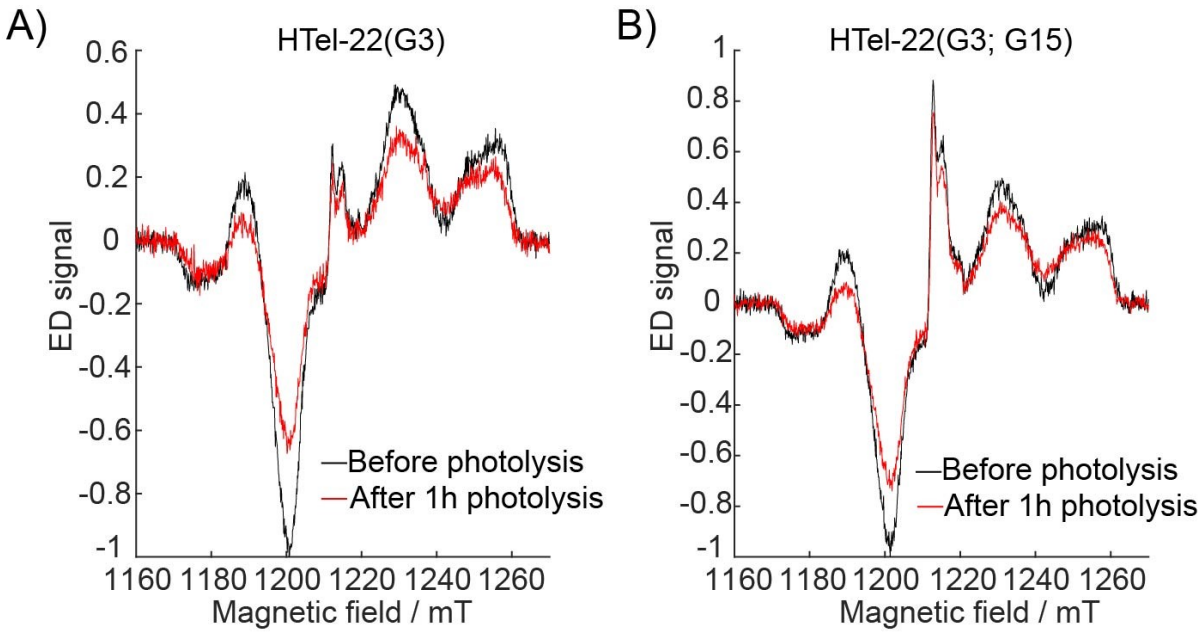

Figure S7. ED spectra of the singly (A) and double (B) labeled HTel-22/TMPyP4 complex ([HTel-22]=50 μM, [TMPyP4]=100 μM) at concentration ratio 1:2 before (black line) and after (red line) photolysis for 60 min at 30 K. All spectra were normalized on maximum ED spectra before photolysis.

6. CW EPR spectra and their simulations

Table S1 shows the reduction of nitroxide spin concentration due to 1-hour photolysis, as obtained from continuous wave (CW) EPR spectra. Figure S8 displays the experimental CW EPR spectra of HTel-22(G3; G15) and HTel-22(G3) complexes with TMPyP4, as well as their simulated spectra calculated in the Easyspin [www.easyspin.org] software using the slow-motion regime to describe label mobility. Modeling the spectra can be complex due to the high degree of polymorphism and conformational switching of the quadruplex. As a result, several assumptions were made to fit the experimental spectra. CW EPR spectra before irradiation were simulated, assuming only one bound fraction with a rotational correlation time (τ_c) of 1.2 ns and anisotropic motion in the orienting potential. After photolysis, we considered the presence of two different fractions (free and bound), characterized by different rotational correlation times of nitroxide and orienting potentials. The free fraction was simulated using τ_c=0.1 ns assuming isotropic motion in the orienting potential. The CW spectra of the TMPyP4/HTel-22(G3) complex was simulated using the same parameters as for the TMPyP4/HTel-22(G3; G15) complex.

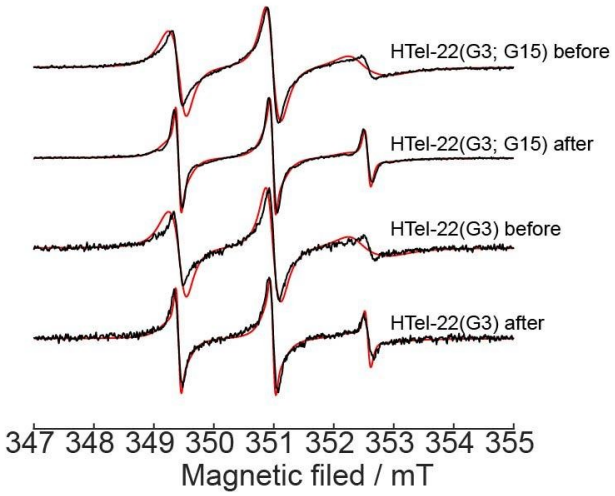

Figure S8. Room-temperature X-band CW EPR spectra for all TMPyP4/spin derivatives HTel-22 complexes and their simulations (red lines) before and after photolysis.

Table S1. The spin concentration of the studied sample

The sample	Before photolysis	After 1h photolysis
TMPyP4/HTel-22(G3)	40 μM	30 μM
TMPyP4/HTel-22(G3; G15)	95 μM	77 μM

Table S2. The parameters for simulations TMPyP4/HTel-22 (G3; G15) CW spectra shown in Fig. S8.

The sample	A [Axx Ayy Azz], MHz	Line width [Gauss Lorentz], mT	τ_c, ns	[$\lambda_{2,0}$ $\lambda_{2,2}$]	g-factor	Fraction weight, %
Before photolysis	[16 16 104]	[0.05 0.05]	1.2	[0.7 -0.7]	[2.0083 2.0061 2.0022]	100
	[16 16 101]	[0.07 0.05]	0.1	[0 0]	[2.0086 2.0061 2.0022]	0
After 1h photolysis	[16 16 104]	[0.05 0.05]	1.2	[0.7 -0.7]	[2.0083 2.0061 2.0022]	86
	[16 16 101]	[0.07 0.05]	0.1	[0 0]	[2.0086 2.0061 2.0022]	14

7. Distance distributions of doubly labeled HTel for parallel and antiparallel conformations of HTel

Figure S9 compares the DEER experimental (A) and predicted (B) distance distributions of the double-labeled TMPyP4/HTel-22 (G3:G15) complex, as calculated using the DeerNet software in this study and data from reference [2].

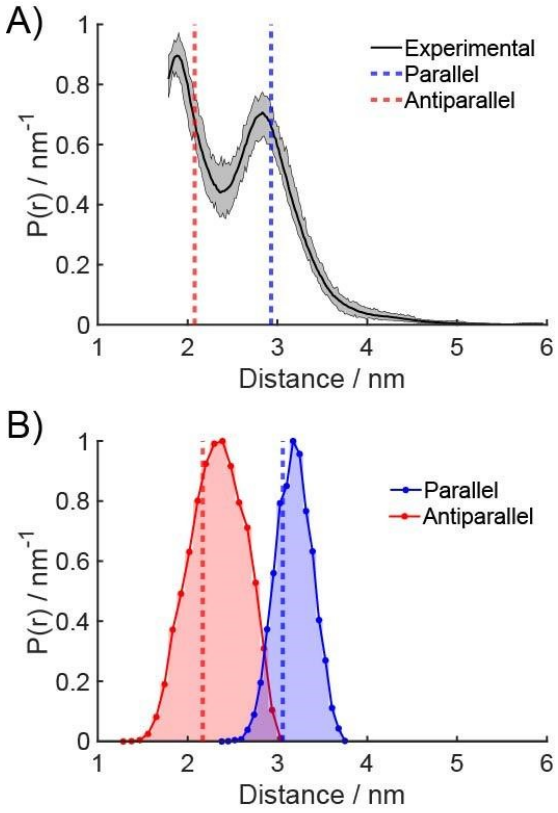

Figure S9. DEER measurements of double labeled TMPyP4/ HTel-22 (G3:G15) complex. A) Normalized on modulation depth computed by the use of DEERNet distance distribution with uncertainty margins. Dashes lines indicate obtained experimental distances in ref [2]. B) Histogram plots of the statistical distributions of the inter-spin distances for parallel and antiparallel conformations. Dashes lines show average predicted distances in ref [2].

8. ReLaserIMD distance distributions of singly labeled HTel-22 for different conformations of HTel-22 and positions of porphyrin

Figure S10 compares the ReLaserIMD experimental (black line) and predicted (colored lines with areas) distance distributions of the singly-labeled TMPyP4/HTel-22 (G3) complex between the nitroxide label and the photoexcited triplet state of TMPyP4, calculated using the Chilife and MDAnalysis Python packages.

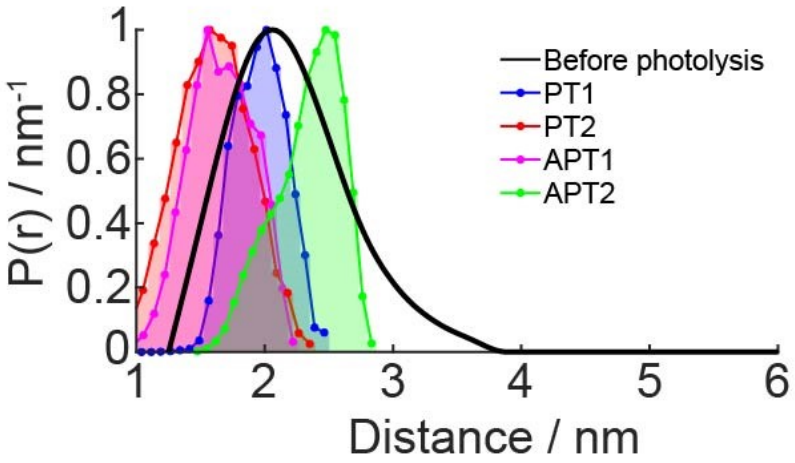

Figure S10. The experimental distance distribution before photolysis (black) of TMPyP4/ HTel-22(G3) complex and calculated histograms with envelope curves of predicted distance distributions in parallel (blue and red) and antiparallel (magenta and green) conformations for different positions of TMPyP4.

REFERENCES

1 D. R. Kattnig, J. Reichenwallner and D. Hinderberger, Modeling excluded volume effects for the faithful description of the background signal in double electron-electron resonance, *J. Phys. Chem. B*, 2013, **117**, 16542–16557.

2 Zhang, X.; Xu, C. X.; Di Felice, R.; Sponer, J.; Islam, B.; Stadlbauer, P.; Ding, Y.; Mao, L.; Mao, Z. W.; Qin, P. Z. Conformations of Human Telomeric G-Quadruplex Studied Using a Nucleotide-Independent Nitroxide Label. *Biochemistry* **2016**, *55* (2), 360–372. https://doi.org/10.1021/ACS.BIOCHEM.5B01189.